

# On the nature of compact stars determined by gravitational waves, radio-astronomy, x-ray emission and nuclear physics

H. Güven

*Université Paris-Saclay, CNRS/IN2P3, IJCLab, 91405 Orsay, France and  
Physics Department, Yildiz Technical University, 34220 Esenler, Istanbul, Turkey*

J. Margueron

*Univ Lyon, Univ Claude Bernard Lyon 1, CNRS/IN2P3,  
IP2I Lyon, UMR 5822, F-69622, Villeurbanne, France*

K. Bozkurt

*Physics Department, Yildiz Technical University, 34220 Esenler, Istanbul, Turkey and  
Université Paris-Saclay, CNRS/IN2P3, IJCLab, 91405 Orsay, France*

E. Khan

*Université Paris-Saclay, CNRS/IN2P3, IJCLab, 91405 Orsay, France and  
Institut Universitaire de France (IUF)*

(Dated: April 3, 2023)

We investigate the question of the nature of compact stars, considering they may be neutron stars or hybrid stars containing a quark core, within the present constraints given by gravitational waves, radio-astronomy, X-ray emissions from millisecond pulsars and nuclear physics. A Bayesian framework is used to combine together all these constraints and to predict tidal deformabilities and radii for a  $1.4 M_{\odot}$  compact star. We find that present gravitation wave and radio-astronomy data favors asy-stiff EoS compatible with nuclear physics and that GW170817 waveform is best described for binary hybrid stars. In addition, this data favors stiff quark matter, independently of the nuclear EoS. Combining this result with constraints from X-ray observation supports the existence of canonical  $1.4 M_{\odot}$  mass hybrid star, with a radius predicted to be  $R_{1.4} = 12.02(8)$  km.

Neutron Stars (NSs), and most generally compact stars (CSs), are forefront laboratories to explore the properties of extreme matter and consequently the strong interaction. The guidance of experimental and observational data are of prime importance, especially because the theory of the strong interaction, the quantum chromodynamics (QCD), could not be simply applied in the regime explored by CSs. One of the most important question in this field is to understand how the strong interaction evolves as function of the density and how quark matter emerges from hadrons [1, 2], if it ever does for densities relevant for stable CSs. Therefore, one should consider two types of CS: NS, with no phase transition in the core, and hybrid stars (HS), with phase transition, towards quark matter, in the core. Note that the existence of strange quark stars is not considered in our analysis since we assume that matter is ruled by a single equation of state. In the present paper, we investigate the onset of a first order phase transition (FOPT) producing the largest correction to the global properties of CSs. It should be noted that CSs observations are also complementary to Earth experiments, such as for instance heavy ion collision [3], since they explore very isospin asymmetric and dense matter.

Over the last decade, the observation of CSs has entered into the era of precision measurements, which provides unprecedented possibilities for constraining the EoS. Among these constraints, the most impactful ones are shown in Fig. 1: The detection of massive NSs by ra-

dio astronomers has pushed up the maximum mass limit, which is presently around  $2M_{\odot}$  [6, 10–14]. As a typical example, the maximum mass limit from J0348+0432 [6] is shown in Fig. 1. In addition to the masses, the radii of a few millisecond pulsars (PSR J0030+0451 [7, 15] and PSR-J0740+6620 [8, 16]) have recently been extracted from X-rays observations, using NICER observatory [17]. Finally, the event GW170817 [18–20], produced by the merger of two CSs, allowed the first estimation of the effective tidal deformability  $\bar{\Lambda}$  for dense matter [21–23], which is shown in the right panels in Fig. 1.

The link between the observation of CSs and the strong interaction is performed through the equation of state (EoS), i.e., the pressure  $p$  versus the energy density  $\varepsilon$ . By solving the Tolman-Oppenheimer-Volkoff (TOV) equations for spherical non-rotating and non-magnetized stellar objects [24, 25], the EoS can be transformed into observational CS properties, e.g., a relation between masses and radii. For such kind of direct comparison, it is important to accurately estimate systematical uncertainties. This can be performed for instance by solving the TOV equations for a large set of EoSs compatible with the current knowledge. In this way, the model uncertainties in the EoS can be turned into a contour in the macroscopic properties, e.g., masses, radii and tidal deformabilities, shown in Fig. 1. The tidal deformability is well correlated to the compactness ( $\beta = M/R$ ) of the compact star [18], and together with the measure of the mass extracted from the gravitational waveform, it allows

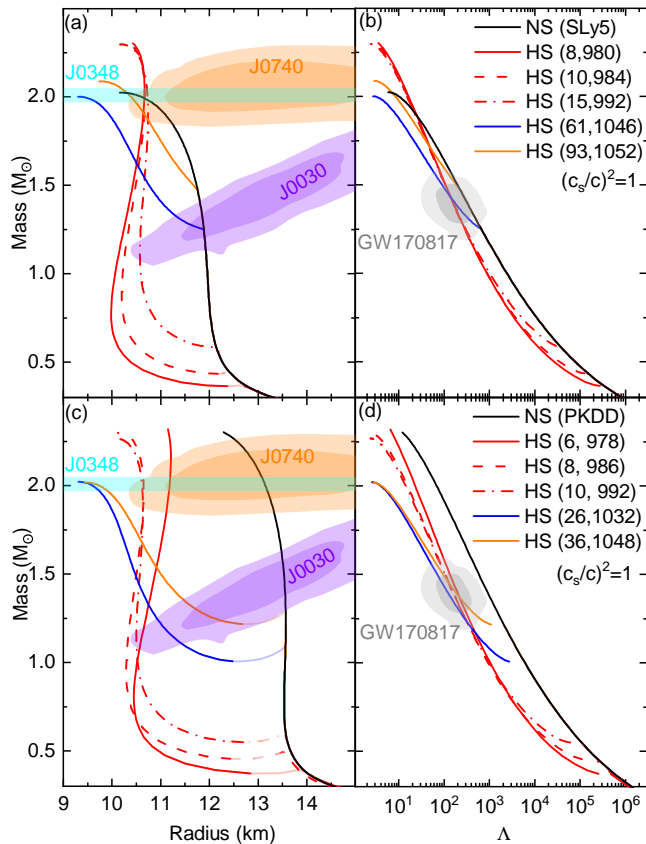


FIG. 1: Mass-radius (left) and mass-tidal deformability (right) representations for SLy5 [4] (top) and PKDD [5] (bottom). The observational contours are related to the analysis of: J0348+0432 [6], J0030+0451 [7], J0740+6620 [8], and GW170817 [9]. The lines represent predictions of a few selected EoS: purely nucleonic EoS for NS (black and solid lines), and the others (color lines) show examples of FOPT built upon nucleonic EoS considering the maximally stiff case ( $c_s = c$ ) for the quark phase. The FOPT parameters  $p_{PT}$  (MeV fm $^{-3}$ ) and  $\mu^*$  (MeV) are given in the inset for HS.

to infer the value of the radius [20, 26]. In some analyses, it is the radius prediction inferred from the tidal deformability, assuming agnostic EoS modeling or universal relations, which is directly used to select EoS models [27].

A few examples of NS and HS EoSs are shown in Fig. 1, comparing predictions based on the nucleonic SLy5 [4] (top panel) and PKDD [5] (bottom panel) EoSs. We employ in this study these two typical nucleonic EoS which differ by the density dependence of the symmetry energy: we consider an isospin soft model, hereafter called asy-soft, represented by SLy5 [4] nuclear model and an isospin stiff model, called asy-stiff, represented by PKDD [5] relativistic Lagrangian. The choice of reducing the nuclear EoS to only two typical ones is also performed by other authors, see for instance Ref. [28].

The SLy5 model is compatible with recent chiral EFT predictions with a low value of the slope of the symmetry energy ( $L_{\text{sym}} = 48.3$  MeV) [29, 30], as well as with the analysis of the PREX-II experiment including also binding energies, charge radii and dipole polarisabilities in a set of finite nuclei [31]. The asy-stiff PKDD model ( $L_{\text{sym}} = 79.5$  MeV) is compatible with another analysis of PREX-II experiment [32].

Note that all the EoSs considered here satisfy the current experimental, theoretical and observational constraints that we detail in this study. Twin stars, i.e., two stars with same mass but different radii, may exist [33] but, in the present study, they are not considered since we impose a one-to-one correspondence between masses and radii.

By showing models and observational contours, Fig. 1 illustrates that it is difficult to find equations of state which reproduce equally well the contours from NICER observatory (left panels) and from GW170817 (right panel). For instance PKDD is out of the GW170817 contour but it is in very good agreement with the two other contours from NICER observatory. The opposite is observed for the other models which reproduce well GW170817. This tension has already been observed in previous studies, see for instance Refs. [34–37]. Because of this tension in the data, we adopt the common strategy: we employ GW170817 to select EoSs, by comparing different kind of binary systems: binary neutron stars (BNS), binary hybrid stars (BHS) and neutron star hybrid star (NSHS). This allows to determine whether one of these system is favored, in a Bayesian framework, by the present data. In a second step, we combine the prediction of these modelings together with NICER contour to infer the radius  $R_{1.4}$  of a  $1.4M_{\odot}$  compact star.

In order to describe hybrid stars, a first order phase transition is built on top of nucleonic EoSs. The quark phase is described by the constant sound speed approach inspired from the MIT bag model [38]. It requires three quantities: the pressure  $p_{PT}$  at the entrance of the phase transition, the shift in energy density, reflecting the latent heat  $\Delta\varepsilon_{PT}$ , and finally, the sound speed  $c_s$  in quark matter assumed to be constant. We have [39–41]:

$$\varepsilon(p) = \begin{cases} \varepsilon_{\text{NM}}(p) & p < p_{PT} \\ \varepsilon_{\text{NM}}(p_{PT}) + \Delta\varepsilon_{PT} + (p - p_{PT})/\alpha & p \geq p_{PT} \end{cases} \quad (1)$$

where  $\varepsilon_{\text{NM}}$  is the nucleonic matter energy density, and  $\alpha$  is related to the sound speed as  $\alpha = (c_s/c)^2$ , where  $c$  is the speed of light in the vacuum. In the following, we use units where  $c = 1$ . A similar approach has recently been employed in [27, 28, 42, 43], leading to the possible existence of a third branch of compact stars [44]. In our study, we use these modeling to explore the nature of CS favored by the present data.

In practice we use the parameters  $p_{PT}$  and  $\mu^*$ , which represents the chemical potential of quark matter at zero pressure, and from which the latent heat  $\Delta\varepsilon_{PT}$  can be

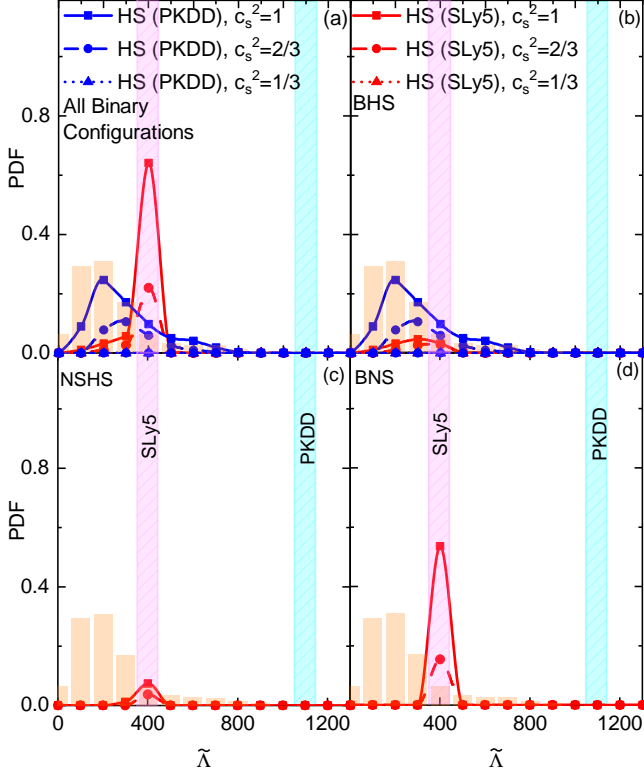


FIG. 2: Posterior PDF function of  $\tilde{\Lambda}$  obtained for BNS, BHS and NSHS configurations. The data shown in the graph is extracted from Ref. [9]. The different line styles correspond to different sound speeds  $c_s^2 = 1/3, 2/3$  and  $1$ . The two vertical bands represent the tidal deformabilities obtained for the purely nucleonic EoSs, see the panel associated to binary configurations.

recovered as

$$\Delta \varepsilon_{\text{PT}} = \frac{p_{\text{PT}}}{\alpha} \left[ \frac{1 + \alpha}{\left[ \frac{\mu_{\text{NM}}(p_{\text{PT}})}{\mu^*} \right]^{\frac{1+\alpha}{\alpha}} - 1} + 1 \right] - \varepsilon_{\text{NM}}(p_{\text{PT}}). \quad (2)$$

We consider the following ranges for the model parameters (priors):  $\mu^* = 925 \pm 75$  MeV, suggested from color-superconducting quark matter calculations [45]; the sound speed parameter  $\alpha$  is fixed to three possible values:  $\alpha = 1/3$  (conformal limit),  $2/3$  and  $1$  (causal limit); and finally,  $p_{\text{PT}}$  is an unconstrained parameter with unknown boundaries. Here, we vary  $p_{\text{PT}}$  from 6 to 500 MeV fm $^{-3}$ , guided by the vanishing of the posterior distribution.

It should be noted that in the present study, quark matter may appear already around (and above) saturation density, since we explore a large space for the sound speed, ranging between  $1/\sqrt{3}$  and  $1$ . While other analyses also explore a large space (see for instance Ref. [27]) which predict quark matter to appear on the average for densities around  $1.5n_{\text{sat}}$ , some analyses of quark mat-

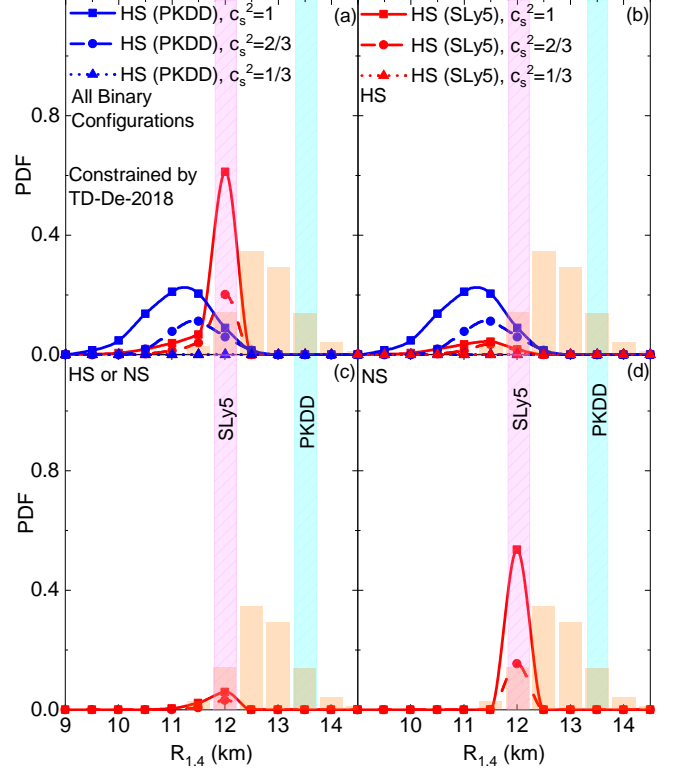


FIG. 3: Same as Fig. 2 but as function of the radius  $R_{1.4}$ . The data shown in the graphs are deduced from the analysis of PSR J0030+0451 by Miller *et al.* [7] where the PDF is sliced for masses between  $1.35$  and  $1.45M_{\odot}$ . The two vertical bands represent the radii obtained from the purely nucleonic EoSs, see the panel associated to binary configurations.

ter predict its appearance above  $3n_{\text{sat}}$  [46] or above  $1.6M_{\odot}$  [47]. These predictions may be related to the choice of the sound speed prior in these analyses.

We employ the Bayesian approach to compare our model predictions, represented by a set of EoS parameters  $\{a_i\}$  with the present data [48]. The probability associated to a given model considering a set of data, the so-called the posterior probability, is

$$P(\{a_i\}|\text{data}) \sim P(\text{data}|\{a_i\}) \times P(\{a_i\}), \quad (3)$$

where  $P(\text{data}|\{a_i\})$  is the likelihood function representing the ability of the model to reproduce a set of measurements and  $P(\{a_i\})$  is the prior probability, which represents the *a-priori* knowledge on the model parameters. We vary the parameters controlling the FOPT,  $\alpha$ ,  $p_{\text{PT}}$  and  $\mu^*$ , which are yet unconstrained parameters. The likelihood probability entering Eq. (3) is defined as,

$$P(\text{data}|\{a_i\}) = w_{\text{filter}}(\{a_i\}) \times p_{\tilde{\Lambda}}, \quad (4)$$

where  $w_{\text{filter}}(\{a_i\})$  is a pass-band type filter which selects only the viable models with maximum mass larger

	EOS	$c_s^2$	BHS	NSHS	BNS
asy-soft	SLy5	1/3	0.00	0.00	0.00
	SLy5	2/3	0.07	0.04	0.07
	SLy5	1	0.12	0.08	0.06
asy-stiff	PKDD	1/3	0.00	0.00	0.00
	PKDD	2/3	<b>0.28</b>	0.00	0.00
	PKDD	1	<b>0.65</b>	0.00	0.00

TABLE I: Overlap between the model prediction and the PDF associated to GW170817, as function of the nucleonic EoS, the sound speed in quark matter and the nature of the binary system. The largest overlaps are stressed in bold.

	EOS	Configuration	$c_s^2$	$R_{1.4}$ Radius
			km	km
asy-soft	SLy5	NS	2/3	12.00(0)
	SLy5	NS	1	12.00(0)
	SLy5	HS	2/3	11.86(6)
	SLy5	HS	1	11.83(6)
	SLy5	HS or NS	2/3	11.98(9)
	SLy5	HS or NS	1	11.96(1)
	Average			11.94(2)
asy-stiff	PKDD	HS	2/3	<b>12.06(12)</b>
	PKDD	HS	1	<b>11.98(11)</b>
	Average			<b>12.02(8)</b>

TABLE II: Predictions for the  $R_{1.4}$  radius constrained by both GW170817 and NICER observation of PSR J0030+0451, as function of the nature of the CS.

than  $2M_\odot$  and  $p_{\tilde{\Lambda}}$  expresses the ability of the model to reproduce the observed probability density function (PDF) for  $\tilde{\Lambda}$  deduced from the GW signal, considering the waveform analysis from Ref. [9]. To do so, the effective tidal deformability  $\tilde{\Lambda}(q)$  is averaged over the mass ratio  $q$  of the binary system in the range  $[0.73, 1]$ , see Ref. [35] for more details.

The posterior probability as a function of the effective tidal deformability  $\tilde{\Lambda}$ , is shown in Fig. 2 for BNS, BHS and NSHS configurations. For BNS systems, only asy-soft EoSs overlap the data since asy-stiff models predict too large tidal deformabilities. NSHS systems are not favored by either asy-soft or asy-stiff EoS. Finally, BHS systems are preferred by asy-stiff models, overlapping at best the data, as shown in Tab. I where bold values mark the best overlaps. In addition, it can be remarked that

the overlap is generally optimal for large sound speed,  $c_s^2 \gtrsim 2/3$ , implying a stiff quark matter phase. Considering Fig. 2 and Tab. I, we conclude that current GW and radio-astronomy observations favors asy-stiff nucleonic EoS compatible with nuclear physics and a BHS configuration for GW170817 event.

The same EoSs are employed to predict  $R_{1.4}$ , as shown in Fig. 3. Independently of their ability to describe GW170817, the two nucleonic EoS compatible with nuclear physics have a good overlap with the NICER data for NSs: they predict radii from 12.00 km (SLy5) to 13.50 (PKDD). But when we condition the model to reproduce GW170817 and radio-astronomy observations, only PKDD survives in the case of HS. Tab. II subsumes the  $R_{1.4}$  predictions conditioned by GW170817, radio-astronomy and nuclear physics. We consider only the cases for which non-zero values are obtained in Tab. I. The centroids are weakly dependent on the nucleonic modelling, going from about 11.8 to about 12.1 km. We obtain however that the asy-stiff EoS, favoring the HS configuration, predicts a radius  $R_{1.4} = 12.02(8)$  km, shown in bold in Tab. II. The asy-soft EoS, which is not favored in Tab. I, predicts a radius  $R_{1.4} = 11.94(2)$  km on average. These two predictions are quite close and considering moreover their uncertainties, they are not significantly different. We then find that the radius of a  $1.4M_\odot$  CS is weakly impacted by the nucleonic EoS as well as by the nature of CS within the two nucleonic scenarios that we have investigated. Considering the present observational data, see Fig. 1 for instance, an uncertainty lower than 100 m in the theoretical prediction for the CSs radius is yet impossible to resolve.

In conclusion, we have obtained that the cross-constraints from gravitational wave, radio-astronomy, x-ray observations and nuclear physics favor binary compact star systems with asy-stiff nucleonic EoS complemented with stiff quark matter. The neutron star-hybrid star configuration is not favored for GW170817 event. The present analysis supports the existence of canonical  $1.4 M_\odot$  mass hybrid star, and illustrates the complementary between nuclear physics and astrophysics for the understanding of dense matter in CS. Future tight constraints in the slope of the symmetry energy  $L_{\text{sym}}$  will further constrain the nature of CSs in GW170817, as well as in the future astrophysical observations, such as for instance binary CS mergers, radio-astronomy or x-ray emission from millisecond pulsars.

This work is supported by the Scientific and Technological Research Council of Turkey (TÜBİTAK) under project number MFAG-122F121 and the Yıldız Technical University under project number FBA-2021-4229. J.M. and E. K. are both supported by the CNRS/IN2P3 MAC project.

[1] M. G. Alford, A. Schmitt, K. Rajagopal, and T. Schäfer, *Rev. Mod. Phys.* **80**, 1455 (2008).

[2] R. Anglani, R. Casalbuoni, M. Ciminale, N. Ippolito,

- R. Gatto, M. Mannarelli, and M. Ruggieri, *Rev. Mod. Phys.* **86**, 509 (2014).
- [3] T. H. Collaboration, *Nat. Phys.* **15**, 1040 (2019).
- [4] E. Chabanat, P. Bonche, P. Haensel, J. Meyer, and R. Schaeffer, *Nucl. Phys. A* **635**, 231 (1998), [Erratum: *Nucl. Phys. A* 643, 441–441 (1998)].
- [5] W. Long, J. Meng, N. V. Giai, and S.-G. Zhou, *Phys. Rev. C* **69**, 034319 (2004).
- [6] J. Antoniadis *et al.*, *Science* **340**, 6131 (2013), arXiv:1304.6875 [astro-ph.HE].
- [7] M. C. Miller, F. K. Lamb, A. J. Dittmann, S. Bogdanov, Z. Arzoumanian, K. C. Gendreau, S. Guillot, A. K. Harding, W. C. G. Ho, J. M. Lattimer, R. M. Ludlam, S. Mahmoodifar, S. M. Morsink, P. S. Ray, T. E. Strohmayer, K. S. Wood, T. Enoto, R. Foster, T. Okajima, G. Prigozhin, and Y. Soong, *The Astrophysical Journal Letters* **887**, L24 (2019).
- [8] M. C. Miller, F. K. Lamb, A. J. Dittmann, S. Bogdanov, Z. Arzoumanian, K. C. Gendreau, S. Guillot, W. C. G. Ho, J. M. Lattimer, M. Loewenstein, S. M. Morsink, P. S. Ray, M. T. Wolff, C. L. Baker, T. Cazeau, S. Manthripragada, C. B. Markwardt, T. Okajima, S. Pollard, I. Cognard, H. T. Cromartie, E. Fonseca, L. Guillemot, M. Kerr, A. Parthasarathy, T. T. Pennucci, S. Ransom, and I. Stairs, *The Astrophysical Journal Letters* **918**, L28 (2021).
- [9] S. De, D. Finstad, J. M. Lattimer, D. A. Brown, E. Berger, and C. M. Biwer, *Phys. Rev. Lett.* **121**, 091102 (2018).
- [10] P. Demorest, T. Pennucci, S. Ransom, M. Roberts, and J. Hessels, *Nature* **467**, 1081 (2010), arXiv:1010.5788 [astro-ph.HE].
- [11] Z. Arzoumanian *et al.* (NANOGrav), *Astrophys. J. Suppl.* **235**, 37 (2018), arXiv:1801.01837 [astro-ph.HE].
- [12] H. T. Cromartie *et al.*, *Nature Astron.* **4**, 72 (2019), arXiv:1904.06759 [astro-ph.HE].
- [13] M. Linares, T. Shahbaz, and J. Casares, *Astrophys. J.* **859**, 54 (2018), arXiv:1805.08799 [astro-ph.HE].
- [14] F. Özel and P. Freire, *Annual Review of Astronomy and Astrophysics* **54**, 401 (2016), <https://doi.org/10.1146/annurev-astro-081915-023322>.
- [15] T. E. Riley *et al.*, *Astrophys. J. Lett.* **887**, L21 (2019), arXiv:1912.05702 [astro-ph.HE].
- [16] T. E. Riley *et al.*, *Astrophys. J. Lett.* **918**, L27 (2021), arXiv:2105.06980 [astro-ph.HE].
- [17] K. Gendreau and Z. Arzoumanian, *Nature Astronomy* **1**, 895 (2017).
- [18] B. P. Abbott, R. Abbott, T. D. Abbott, *et al.* (LIGO Scientific Collaboration and Virgo Collaboration), *Phys. Rev. Lett.* **119**, 161101 (2017), arXiv:1710.05832 [gr-qc].
- [19] B. P. Abbott, R. Abbott, T. D. Abbott, *et al.* (LIGO Scientific Collaboration and Virgo Collaboration), *Phys. Rev. Lett.* **121**, 161101 (2018).
- [20] B. P. Abbott, R. Abbott, T. D. Abbott, *et al.* (LIGO Scientific Collaboration and Virgo Collaboration), *Phys. Rev. X* **9**, 011001 (2019).
- [21] E. E. Flanagan and T. Hinderer, *Physical Review D* **77** (2008), 10.1103/PhysRevD.77.021502.
- [22] T. Hinderer, *The Astrophysical Journal* **677**, 1216 (2008).
- [23] T. Damour and A. Nagar, *Physical Review D* **80** (2009), 10.1103/PhysRevD.80.084035.
- [24] R. C. Tolman, *Phys. Rev.* **55**, 364 (1939).
- [25] J. R. Oppenheimer and G. M. Volkoff, *Phys. Rev.* **55**, 374 (1939).
- [26] I. Tews, J. Margueron, and S. Reddy, *European Journal of Physics A* **55**, 97 (2019).
- [27] W.-J. Xie and B.-A. Li, *Phys. Rev. C* **103**, 035802 (2021).
- [28] S. Han and A. W. Steiner, *Phys. Rev. D* **99**, 083014 (2019).
- [29] C. Drischler, K. Hebeler, and A. Schwenk, *Phys. Rev. Lett.* **122**, 042501 (2019).
- [30] R. Somasundaram, C. Drischler, I. Tews, and J. Margueron, *Phys. Rev. C* **103**, 045803 (2021).
- [31] P.-G. Reinhard, X. Roca-Maza, and W. Nazarewicz, *Phys. Rev. Lett.* **127**, 232501 (2021), arXiv:2105.15050 [nucl-th].
- [32] B. T. Reed, F. J. Fattoyev, C. J. Horowitz, and J. Piekarewicz, *Phys. Rev. Lett.* **126**, 172503 (2021), arXiv:2101.03193 [nucl-th].
- [33] J. J. Li, A. Sedrakian, and M. Alford, *Phys. Rev. D* **107**, 023018 (2023).
- [34] C. D. Capano, I. Tews, S. M. Brown, B. Margalit, S. De, S. Kumar, D. A. Brown, B. Krishnan, and S. Reddy, *Nature Astron.* **4**, 625 (2020), arXiv:1908.10352 [astro-ph.HE].
- [35] H. Güven, K. Bozkurt, E. Khan, and J. Margueron, *Phys. Rev. C* **102**, 015805 (2020), arXiv:2001.10259 [nucl-th].
- [36] P. T. H. Pang, I. Tews, M. W. Coughlin, M. Bulla, C. V. D. Broeck, and T. Dietrich, *The Astrophysical Journal* **922**, 14 (2021).
- [37] H. Dinh Thi, C. Mondal, and F. Gulminelli, *Universe* **7** (2021), 10.3390/universe7100373.
- [38] A. Chodos, R. L. Jaffe, K. Johnson, C. B. Thorn, and V. F. Weisskopf, *Phys. Rev. D* **9**, 3471 (1974).
- [39] Zdunik, J. L. and Haensel, P., *A&A* **551**, A61 (2013).
- [40] M. G. Alford, S. Han, and M. Prakash, *Phys. Rev. D* **88**, 083013 (2013), arXiv:1302.4732 [astro-ph.SR].
- [41] Chamel, N., Fantina, A. F., Pearson, J. M., and Gorieli, S., *A&A* **553**, A22 (2013).
- [42] R. Somasundaram and J. Margueron, *EPL* **138**, 14002 (2022), arXiv:2104.13612 [astro-ph.HE].
- [43] R. Somasundaram, I. Tews, and J. Margueron, *Phys. Rev. C* **107**, 025801 (2023), arXiv:2112.08157 [nucl-th].
- [44] M. Alford and A. Sedrakian, *Phys. Rev. Lett.* **119**, 161104 (2017).
- [45] B. K. Agrawal, *Phys. Rev. D* **81**, 023009 (2010).
- [46] A. Pfaff, H. Hansen, and F. Gulminelli, *Phys. Rev. C* **105**, 035802 (2022).
- [47] A. Parisi, C. V. Flores, C. H. Lenzi, C.-S. Chen, and G. Lugones, *Journal of Cosmology and Astroparticle Physics* **2021**, 042 (2021).
- [48] A. W. Steiner, *Journal of Physics G: Nuclear and Particle Physics* **42**, 034004 (2015).